Molecular Therapy
Original Article

Combination Cancer Therapy Using Chimeric Antigen Receptor-Engineered Natural Killer Cells as Drug Carriers

Elizabeth L. Siegler,[1,4] Yu Jeong Kim,[2,4] Xianhui Chen,[2] Natnaree Siriwon,[3] John Mac,[3] Jennifer A. Rohrs,[1] Paul D. Bryson,[3] and Pin Wang[1,2,3]

[1]Department of Biomedical Engineering, University of Southern California, Los Angeles, CA 90089, USA; [2]Department of Pharmacology and Pharmaceutical Sciences, University of Southern California, Los Angeles, CA 90089, USA; [3]Mork Family Department of Chemical Engineering and Materials Science, University of Southern California, Los Angeles, CA 90089, USA

The therapeutic limitations of conventional chemotherapeutic drugs include chemo-resistance, tumor recurrence, and metastasis. Numerous nanoparticle-based active targeting approaches have emerged to enhance the intracellular concentration of drugs in tumor cells; however, efficient delivery of these systems to the tumor site while sparing healthy tissue remains elusive. Recently, much attention has been given to human immune-cell-directed nanoparticle drug delivery, because immune cells can traffic to the tumor and inflammatory sites. Natural killer cells are a subset of cytotoxic lymphocytes that play critical roles in cancer immunosurveillance. Engineering of the human natural killer cell line, NK92, to express chimeric antigen receptors to redirect their antitumor specificity has shown significant promise. We demonstrate that the efficacy of chemotherapy can be enhanced in vitro and in vivo while reducing off-target toxicity by using chimeric antigen receptor-engineered NK92 cells as carriers to direct drug-loaded nanoparticles to the target site.

INTRODUCTION

Cancer treatments typically include surgical removal, chemotherapy, radiation, or some combination of these therapies.[1] While these methods can remove the majority of the tumor cells, tumor recurrence and metastasis remain a major obstacle in cancer treatment.[2] Solid tumors often do not respond well to traditional anticancer drugs. After relapse, further treatment options frequently include different chemotherapeutics, and the time to progression typically shortens after each relapse.[3] At best, it can be managed as a "chronic" disease for many years, but cumulative toxicities of successive chemotherapy treatments are a serious consideration.

Cancer immunotherapy has gained much attention within the last decade, and more recently, the concept of using immune cells as vehicles to transport anticancer agents directly to the tumor site has gained attention.[4–6] Natural killer (NK) cells are part of the innate immune system and mediate rapid, short-lived responses by releasing perforin and granzymes that directly lyse infected or abnormal cells including tumor cells.[7,8] The NK92 cell line is identical to the parental NK line isolated from a lymphoma patient.[9] NK92 cells are the most extensively characterized and well-documented with antitumor effects against various types of cancer including melanoma, leukemia, and breast cancer in both preclinical and clinical settings.[10–12] NK cells are not specifically cytotoxic to certain antigen-expressing target cells,[13] but their specificity and efficacy can be enhanced with the use of chimeric antigen receptors (CARs). CARs are antigen-specific engineered receptors that can be expressed on human immune cells.[14–16] They are composed of an extracellular antigen-binding domain derived from an antibody fragment.[17] This allows the CAR-expressing immune cells to bind to specific surface antigens overexpressed on cancer cells. Intracellular signaling domains within the CAR provide signals to the immune cell to attack the antigen-expressing cell.[18,19] Typically, CARs are expressed in T cells, but recent studies show that CARs are effective tumor-targeting molecules in NK cells as well.[20–23] The inclusion of CARs in NK92 cells (CAR.NK) increases homing, specificity, and efficacy of tumor killing.

Paclitaxel (PTX) is a common chemotherapeutic that has been used clinically for many years to treat various cancers. However, the therapeutic efficacy and clinical application of PTX is hindered by its hydrophobicity, high toxicity, and low bioavailability. Many studies have shown that nanoparticle formulation of PTX has enhanced its delivery to the tumor site with reduced systemic toxicity as compared with the unmodified free drug.[24–26] For example, Abraxane is a US Food and Drug Administration (FDA)-approved formulation of PTX and albumin nanoparticles that has been shown to significantly increase overall survival in clinical trials compared with free drug administration.[27] Nanoparticles are considered promising drug delivery vehicles for cancer therapy based on their ability

Received 14 June 2017; accepted 15 August 2017;
http://dx.doi.org/10.1016/j.ymthe.2017.08.010.

[4]These authors contributed equally to this work.

Correspondence: Pin Wang, Mork Family Department of Chemical Engineering and Materials Science, University of Southern California, 3710 McClintock Avenue, RTH-506, Los Angeles, CA 90089, USA.
E-mail: pinwang@usc.edu

to increase drug accumulation at tumor sites via the enhanced permeability and retention (EPR) effect. The EPR effect describes a phenomenon in which irregular, leaky vasculature and poor lymphatic drainage within a tumor allow larger nanoparticles to extravasate and remain in the tumor site.[28] Although the EPR effect has been well-characterized in preclinical models, this mechanism is heterogeneous and may be completely lacking in some tumors.[29] Tumor vasculature heterogeneity often results in nanoparticle accumulation in the extracellular matrix proximal to the tumor vasculature. Tumor cells that are distant from well-defined vasculature are not effectively targeted by these nanoparticles. Moreover, because hypoxic tumor regions have dysregulated tumor vasculature, traditional passive drug targeting via nanoparticles is insufficient.[27] New strategies are desired to guide nanoparticles to poorly vascularized tumor tissue.

Immune cells are an attractive option for active cancer therapeutic delivery because of their natural ability to home to or accumulate at tumor sites.[4] Instead of relying on passive delivery, immune cells can be used as active carriers for nanoparticles that are either directly cytotoxic to the tumor or nanoparticles that carry chemotherapeutic agents. Nanoparticles can be conjugated to the cell surface by directly utilizing functional groups such as amino or thiol groups, through hydrophobic insertion into the lipid bilayer, by electrostatic interactions, or by attaching to specific cell surface receptors.[30] Within the past decade, research groups have demonstrated that nanoparticles delivered by cells can enhance antitumor effects.[31] In many of the current cell-based nanotherapies, the cell serves as a carrier for nanoparticles and their cargo. Tumor-associated antigen (TAA)-targeted T cells have been shown to carry adsorbed oncolytic viruses to tumor sites in several studies,[32–34] and this concept has been extended to synthetic nanoparticle delivery. However, more studies of lymphocytes conjugated to synthetic drug-loaded nanoparticles are needed. Although other immune cell types have been exploited as drug carriers, to our knowledge, NK cells have not been surface engineered with drug-loaded nanoparticles, despite their ability to gather at the tumor site.

To address such a need, we hypothesized that the efficacy of chemotherapy could be enhanced if tumor-specific NK cells were used as carriers to deliver drug-loaded nanoparticles. Based upon the strategies presented in previous studies,[35] we modified our tumor-specific CAR.NK cells with cross-linked multilamellar liposomal vesicles (cMLVs) containing PTX. These cMLVs are liposomes functionalized with thiol-reactive maleimide head groups,[36,37] which allow them to be stably conjugated to the thiol-rich NK cell surface.[35,38] Previously, we have demonstrated that cMLVs can act as a novel agent for combinatory drug delivery by co-localizing two drugs with distinct physicochemical properties to a single site, inducing a synergistic anti-tumor effect in vitro and in vivo.[39,40] Here, our work presents the combination of immunotherapy and chemotherapeutic drug delivery by utilizing CAR.NK cells as carriers for PTX-loaded cMLVs (cMLV[PTX]) to enhance antitumor efficacy in Her2- and CD19-overexpressing cancer models (Figure 1A).

RESULTS

Anti-CD19 and Anti-Her2 CARs Are Expressed in NK92 Cells

We confirmed the ability of NK92 cells to express anti-CD19 and anti-Her2 CARs, which consisted of a single-chain variable fragment (scFv)-derived antigen binding domain, CD8 hinge and transmembrane region, CD28 and/or 4-1BB costimulatory domains, and CD3ζ signaling domain. Anti-CD19 CAR.NK cells were generated with retroviral transduction using the previously documented MP71 vector[41] generously provided by Dr. Wolfgang Uckert. The anti-Her2 CAR.NK cells were generated with lentiviral transduction using a previously described trastuzumab-derived CAR[42] in a pCCW vector, which is based off the pCCL vector[43–45] with an added woodchuck posttranscriptional regulatory element (WPRE) region. Transduced cells were sorted using fluorescence-activated cell sorting to further increase the percentage of CAR^+ cells (Figure S1). CAR expression was stable several months after initial transduction and sorting (data not shown).

cMLVs Are Stably Conjugated to the NK Cell Surface

Previous studies have shown that cross-linked multilamellar liposomal vesicles (cMLVs) were successfully incorporated with both hydrophobic and hydrophilic drugs. As previously illustrated,[46] these vesicles were synthesized through covalently cross-linking functionalized head groups of adjacent lipid bilayers using the conventional dehydration-rehydration method. Synthesized cMLV nanoparticles were stably conjugated to the reduced thiol groups present on the surface of NK cells via the thiol-reactive maleimide head groups present on the lipid bilayer surface. According to previous studies,[5] high levels of free thiols were detected on the surfaces of lymphocytes. The conjugation was performed in two steps. First, NK cells and cMLVs were coincubated to induce particle coupling to free thiols on the cell surface. After the initial reaction, the cMLV-conjugated cells underwent in situ PEGylation to quench residual thiol-reactive groups. To determine the maximum numbers of particles that could be conjugated per NK cell, we performed a serial dilution of the conjugation at different fluorescent-labeled cMLVs-to-cell ratios (2,000:1, 1,000:1, 500:1, 100:1, and 10:1). Between the conjugation ratio of 2,000:1 and 1,000:1, the number of conjugated liposomes per cell began to plateau and showed an average conjugation of approximately 150 nanoparticles per cell (Figure 1B). From these data, we determined that the optimal ratio to use was 1,000:1, because further increasing it did not increase the number of conjugated cMLVs on the cell surface. We used this ratio for all subsequent experiments. Confocal imaging was used to confirm and visualize the conjugation of cMLVs to the NK cell surface (Figure 1C; Figure S2).

As previously reported,[4,35] the major advantages of extended surface retention of nanoparticles on the surface of carrier cells are as follows: (1) prevention from immediate particle degradation because of internalization into degradative intracellular compartments; and (2) sustained drug release from the particle-conjugated cells, which allows for effective targeting of the drug to tumor cells. Several studies

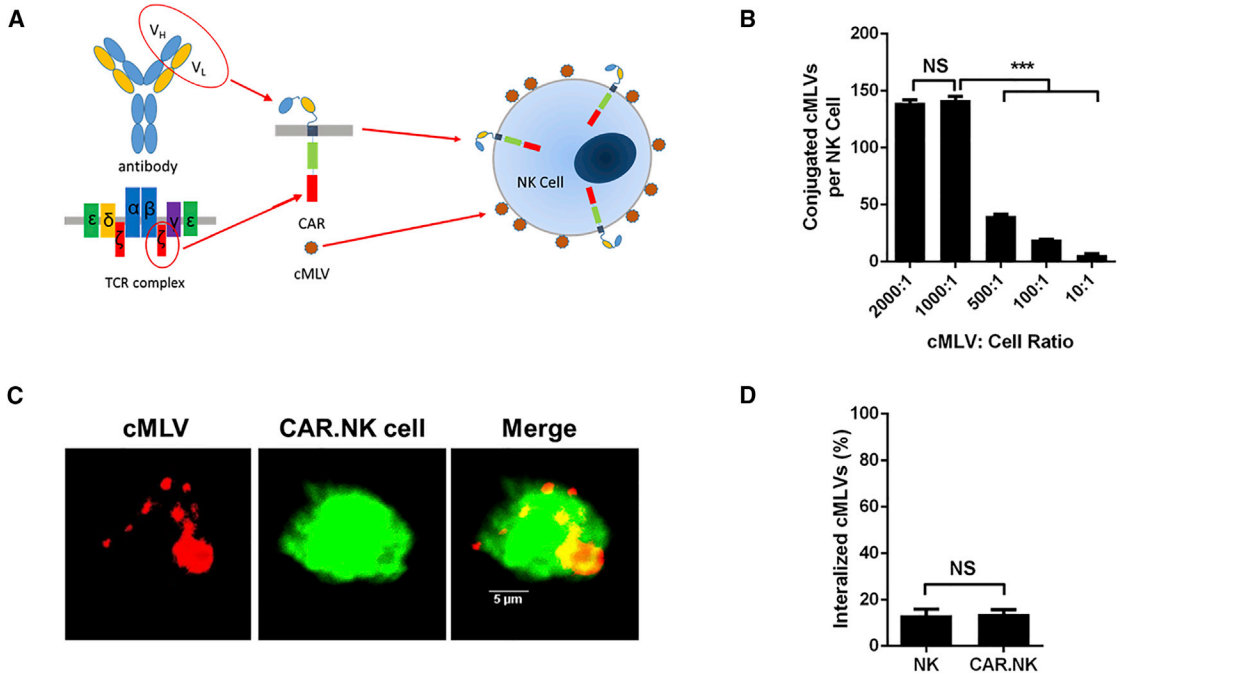

Figure 1. NK92 Cell Conjugation to Maleimide-Functionalized cMLVs

(A) Schematic of CAR.NK cells conjugated to PTX-loaded cMLVs. CARs are derived from the single-chain variable fragment (scFv) of an antibody and the T cell receptor signaling complex. CARs can be transduced into NK92 cells, and cMLVs can conjugate to the cell surface by interacting with free thiols. (B) cMLVs conjugated to the NK cell surface at various cMLV:cell ratios. cMLVs containing the fluorescent dye DiD were coincubated with NK cells over a range of ratios. The number of cMLVs on the surface of each cell was calculated by analyzing the DiD fluorescence. The ratio of 1,000:1 provided the maximum amount of cMLVs per cell and was used in future experiments. (C) Confocal microscopy of CAR.NK cells conjugated to DiD-loaded cMLVs [cMLV(DiD)]. CAR.NK cells were labeled with 1 μM CFSE and washed with PBS prior to conjugation to cMLV(DiD). Confocal microscopy was used to visualize the cMLVs on the CAR.NK cell surface. Scale bars, 5 μm. (D) Internalization assay of conjugated cMLVs. CAR.NK cells were conjugated with carboxyfluorescein-tagged maleimide-labeled cMLVs. The extracellular conjugation was quenched by trypan blue to differentiate surface-bound and internalized cMLVs 2 hr after conjugation. Attachment of cMLVs to CAR.NK cells did not trigger the internalization of particles by the cells. Summarized statistics are displayed in the graphs (n = 3, mean ± SEM; ***$p < 0.001$). NS, not significant.

have shown that nanoparticles can be endocytosed by a variety of cells,[47] including endothelial cells[48,49] and macrophages.[50] However, for our study, it is crucial that the cMLVs remain on the NK cell surface. To address this concern, we performed an experiment to determine the internalization of these particles after conjugation. To determine whether these NK cells could also trigger liposome endocytosis, we conjugated NK cells with cMLVs tagged with a PE CF [1,2-dioleoyl-sn-glycero-3-phosphoethanolamine-*N*-(carboxyfluorescein)] fluorescein dye, then warmed the cells to 37°C and assessed cell-associated fluorescence over time. Attachment of cMLVs to NK cells did not trigger cell uptake of these particles, and particles bound to NK cells remained at the cell surface as shown in Figure 1D.

CAR.NK Cells Have Greater Cytotoxic Effects against Antigen-Expressing Target Cells In Vitro and Are Less Sensitive to PTX

We assessed the ability of CAR.NK cells to trigger cytotoxic effects against the appropriate antigen-expressing target cells by coincubating nontransduced NK or CAR.NK cells with various target cell lines and reading the results with flow cytometry. We used lentivirus to transduce SKOV3 cells to express CD19 (SKOV.CD19) to serve as target cells for our anti-CD19 CAR.NK cells. Both CD19- and Her2-targeting CAR.NK cells demonstrated significantly greater cytotoxicity against the antigen-expressing target cells (SKOV.CD19 and SKOV3, respectively) compared with either nontransduced NK cells or CAR.NK cells coincubated with target cells that did not express the cognate antigen (SKOV3 and MDA.MB.468, respectively; Figures 2A and 2B). These trends were observed at all effector-to-target ratios ($p < 0.01$ for 1:1 and 10:1; $p < 0.001$ for 5:1) and indicated CAR-mediated cell killing.

Because NK92 cells originate from a patient with NK cell lymphoma, these allogenic cells are irradiated prior to clinical use to prevent them from proliferating in vivo.[13,51] In accordance with previous reports,[22,51–53] irradiation did not affect the cytotoxic capabilities of our CAR.NK cells (Figure S3). We also performed a cell viability assay to demonstrate that SKOV3 cells were more sensitive to PTX than were NK cells (Figure S4). This ensures that the NK cells can carry enough PTX to kill target cells without succumbing to PTX-induced toxicity themselves. cMLVs conjugated to NK cells also release the majority of their PTX payload by day 3 (Figure S5).

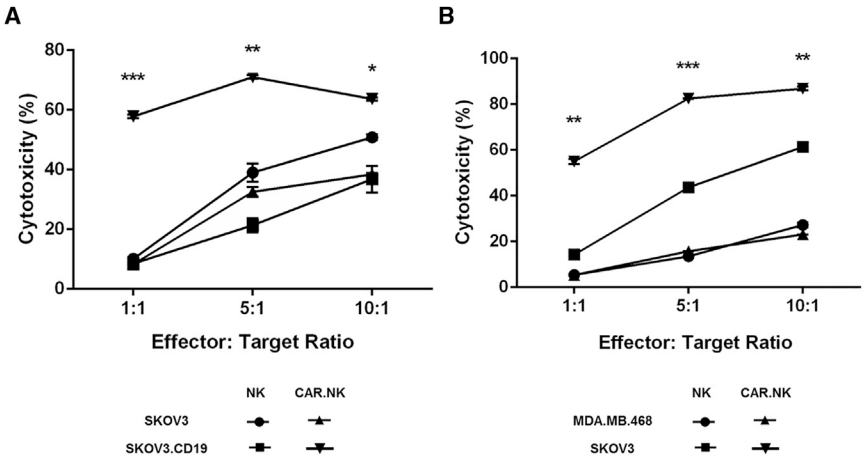

Figure 2. Cytotoxicity of CAR.NK Cells against CD19$^+$ or Her2$^+$ Target Cells

(A) Cytotoxicity of anti-CD19 CAR.NK cells. Anti-CD19 CAR.NK cells were cocultured with CD19$^-$ SKOV3 cells or CD19$^+$ SKOV.CD19 cells for 24 hr at 1:1, 5:1, or 10:1 effector-to-target ratios, and cytotoxicity was measured. (B) Cytotoxicity of anti-Her2 CAR.NK cells. Anti-Her2 CAR.NK cells were cocultured with Her2$^-$ MDA.MB.468 cells or Her2$^+$ SKOV3 cells for 24 hr at 1:1, 5:1, or 10:1 effector-to-target ratios, and cytotoxicity was measured. Summarized statistics are displayed in the graphs (n = 3; mean ± SEM; *p < 0.05; **p < 0.01; ***p < 0.001). NS, not significant.

CAR.NK Function Is Unaffected by cMLV Conjugation and Enhanced with cMLV(PTX) Conjugation In Vitro

We ensured that the conjugation of cMLVs to the CAR.NK cell surface does not affect the functionality of the CAR.NK cell itself. To detect NK cell activation upon antigen binding, we performed an interferon (IFN)-γ release assay, coculturing various target cell lines with NK cells with or without cMLV conjugation. None of the CAR.NK cells reacted when incubated alone or when cocultured with target cells without the cognate antigen, but coincubation with the correct antigen-expressing target cells resulted in significantly greater percentages of IFN-γ$^+$ cells from both anti-CD19 and anti-Her2 CAR.NK cell lines ($p < 0.05$) demonstrating specificity toward the appropriate TAA. When the CAR.NK cells were conjugated to either empty cMLVs containing no drug [CAR.NK.cMLV(EMPTY)] or PTX-loaded cMLVs [CAR.NK.cMLV(PTX)], IFN-γ release was not significantly different from that of unconjugated CAR.NK cells (Figures 3A and 3B).

We repeated the cytotoxicity assays using an effector-to-target ratio of 1:1 with CAR.NK cells that were unconjugated, conjugated to empty cMLVs [CAR.NK.cMLV(EMPTY)], or conjugated to PTX-loaded cMLVs [CAR.NK.cMLV(PTX)]. CAR.NK.cMLV(EMPTY) did not significantly affect TAA$^+$ target cell killing ($p > 0.05$), but cytotoxicity against TAA$^+$ target cells was significantly increased with CAR.NK.cMLV(PTX) ($p < 0.05$ for both CD19 and Her2 models). Significantly greater percentages of TAA$^+$ target cells were killed compared with TAA$^-$ target cells when exposed to CAR.NK.cMLV(PTX) ($p < 0.01$ for the CD19 model; $p < 0.001$ for the Her2 model), confirming that antigen expression by target cells is crucial to enhancing cytotoxicity. The difference in cytotoxicity between cMLV(EMPTY) and cMLV(PTX) was also statistically significant in TAA$^-$ target cells ($p < 0.01$ for the CD19 model; $p < 0.05$ for the Her2 model), indicating that PTX boosts cytotoxicity even without CAR signaling (Figures 3C and 3D). These data indicate that although empty cMLVs do not affect CAR.NK function, the release of PTX from cMLVs in proximity to the target cells boosted cytotoxic effects, which was further enhanced by a CAR-mediated response against TAA$^+$ target cells.

Finally, we monitored NK migration with or without cMLV conjugation. In order to affect an antitumor response, NK cells must extravasate into and migrate within the tumor site in response to chemoattractants.[54] To ensure that cMLV conjugation to the NK surface did not impact cell migration, we performed NK cell transmigration assays. The chemoattractant CXCL9 was used to promote NK cell migration to the lower chamber of the wells. There were significantly more migrated NK cells in the lower chamber when CXCL9 was used as an attractant compared with the plain media control ($p < 0.05$), but there was no significant difference between conjugated and unconjugated groups, indicating that conjugation of either empty or PTX-loaded cMLVs to the cell surface did not impact NK migratory abilities (Figure 3E).

CAR.NK.cMLV Enhances Delivery of cMLVs to the Tumor Site

After confirming the functionality of our cMLV(PTX)-conjugated CAR.NK cells in vitro, we performed a biodistribution study to determine whether CAR.NK cells enhanced cMLV homing to the tumor site. The fluorescent dye 1,1-dioctadecyl-3,3,3,3-tetramethylindodicarbocyanine (DiD) was used to tag cMLVs [cMLV(DiD)] and track their presence in various organs. Non-obese diabetic (NOD)/severe combined immunodeficiency (SCID)/IL2rγ$^{-/-}$ NSG) mice were subcutaneously injected with SKOV.CD19 cells. Two weeks after tumor inoculation, mice were intravenously injected with cMLV(DiD) or conjugated CAR.NK.cMLV(DiD). Mice were sacrificed and organs were analyzed for fluorescence signal at various time points. At 24 hr (Figures 4A and 4B), most of the cMLVs from both groups were still circulating in the blood. The CAR.NK.cMLV(DiD) group had significantly more cMLVs in the blood ($p < 0.001$), lymph node ($p < 0.05$), and tumor ($p < 0.01$), whereas the cMLV(DiD) group had significantly more accumulation in the liver ($p < 0.001$). At 48 hr (Figures 4C and 4D), most of the cMLV(DiD) group had accumulated in the liver, but the CAR.NK.cMLV(DiD) group had significantly more cMLVs in the blood, lymph node, spleen, and tumor ($p < 0.001$). By 72 hr (Figures 4E and 4F), most of the cMLV(DiD) signal was gone, with only small amounts detectable in the liver, blood, and tumor. In contrast, the CAR.NK.cMLV(DiD) group had significantly more cMLVs in the blood, lymph node, spleen, and tumor ($p < 0.001$). Overall, cMLV(DiD) without a cell acting as a chaperone were likely

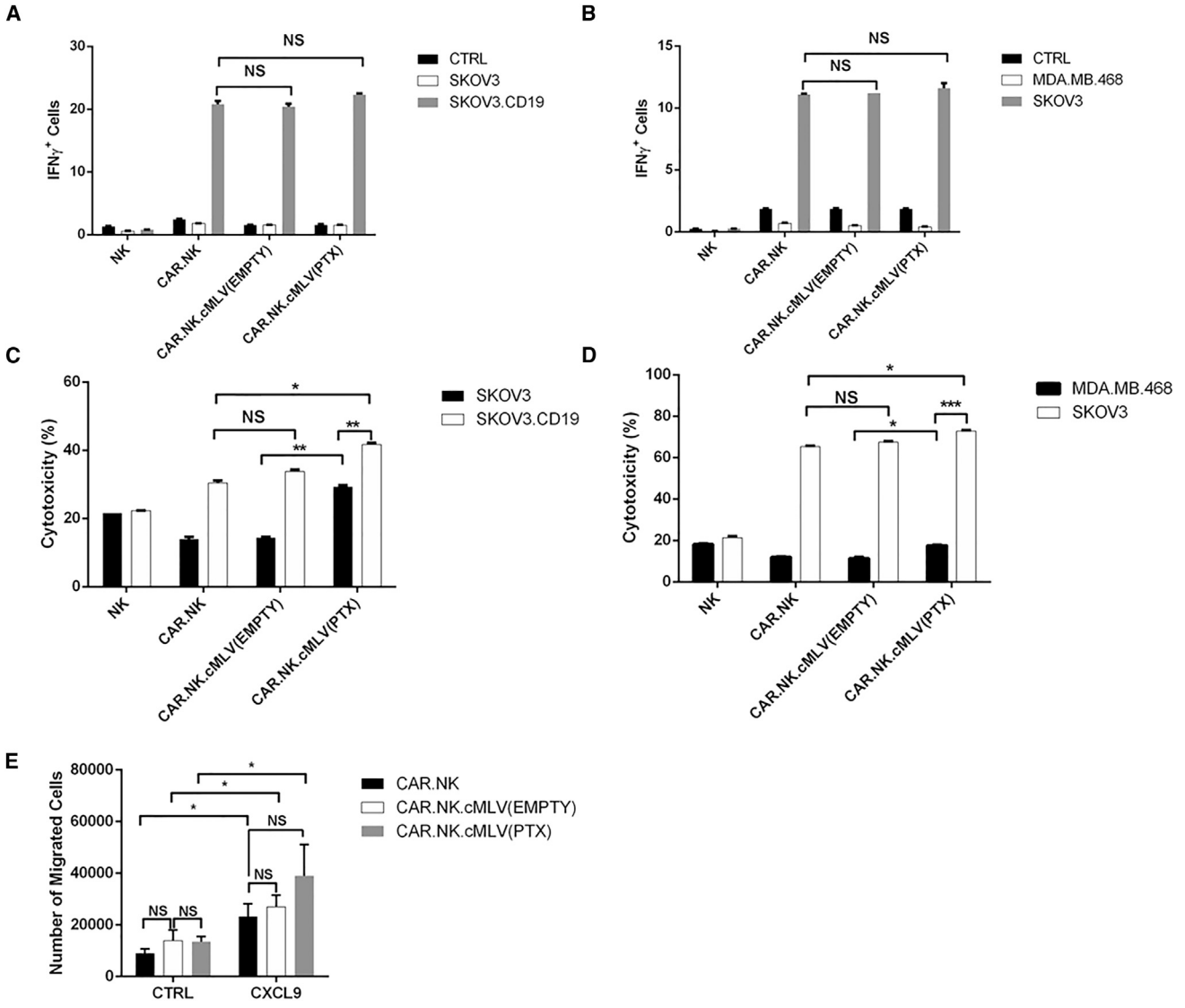

Figure 3. CAR.NK Cytokine Release and Migration When Conjugated to cMLVs

(A and B) IFN-γ staining assays. Anti-CD19 (A) or anti-Her2 (B) CAR.NK cells were cocultured with various target cells with brefeldin A protein transport inhibitor for 6 hr to detect IFN-γ release. Unstimulated CAR.NK cells served as a negative control. CAR.NK cells were either unconjugated or conjugated with empty cMLVs [CAR.NK.cMLV(EMPTY)] or PTX-loaded cMLVs [CAR.NK.cMLV(PTX)]. IFN-γ was measured with intracellular staining. (C and D) Cytotoxicity assays. Anti-CD19 (C) or anti-Her2 (D) CAR.NK cells were cocultured with various target cells at a 1:1 ratio for 24 hr, and cytotoxicity was measured. CAR.NK cells were either unconjugated or conjugated with empty cMLVs [CAR.NK.cMLV(EMPTY)] or PTX-loaded cMLVs [CAR.NK.cMLV(PTX)]. (E) Migration assay. Unconjugated NK or NK conjugated to cMLV(EMPTY) or cMLV(PTX) were plated in the upper chambers of a Transwell plate. Negative controls had plain media in the lower wells, and CXCL9 was used as a chemoattractant in the lower wells of non-control groups. After 6 hr of incubation, media from the lower chambers were collected and NK cells were counted. Summarized statistics are displayed in the graphs (n = 3; mean ± SEM; *p < 0.05; **p < 0.01; ***p < 0.001). NS, not significant.

cleared by the liver, because hepatic clearance serves as the main clearance route for particles too large to be cleared by the kidneys.[55,56] In contrast, cMLV(DiD) that were conjugated to CAR.NK cells were able to home to the tumor site.

CAR.NK.cMLV(PTX) Enhances Antitumor Efficacy In Vivo

We established a mouse xenograft model to observe the effects of the anti-CD19 CAR.NK cells in vivo. NSG mice were subcutaneously injected with SKOV.CD19 cells. Two weeks after tumor inoculation, mice were randomly divided into six groups and injected with: (1) PBS as a control; (2) cMLV(PTX) only, without any cellular component; (3) nontransduced NK cells only; (4) CAR.NK cells only; (5) mixed cMLV(PTX) + CAR.NK, which were coinjected but not conjugated; and (6) conjugated CAR.NK.cMLV(PTX) cells. Mice treated with CAR.NK.cMLV(PTX) had significantly slowed tumor growth compared with PBS, cMLV(PTX), and NK groups ($p < 0.001$), and

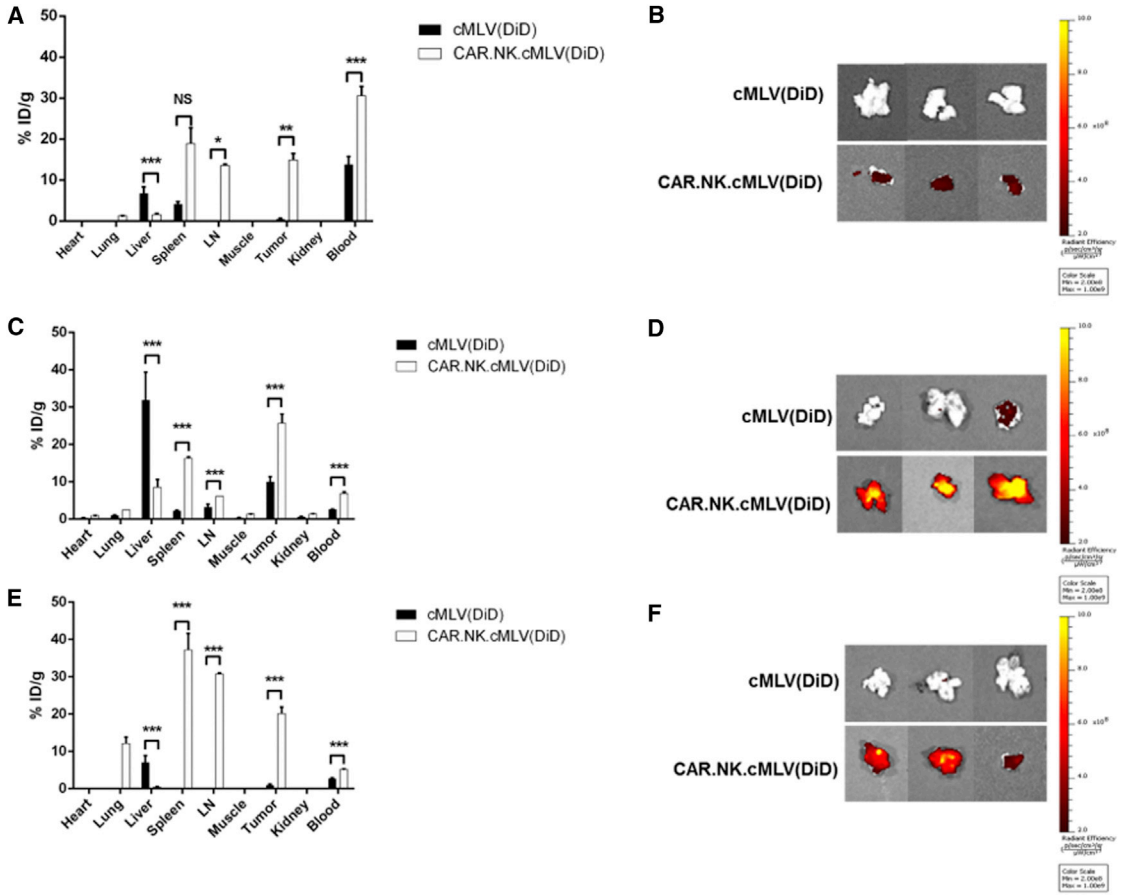

Figure 4. Biodistribution of Free cMLV(DiD) and Conjugated CAR.NK.cMLV(DiD)

(A–F) Biodistribution data 24 (A and B), 48 (C and D), or 72 hr (E and F) after intravenous injections. NOD/SCID/IL2rγ$^{-/-}$ (NSG) mice bearing subcutaneous SKOV3.CD19 tumors were intravenously injected with 2 × 10^7 CAR.NK cells conjugated with DiD-labeled cMLVs or an equivalent number of DiD-labeled cMLVs alone (n = 3 per group per time point). After 24, 48, and 72 hr, indicated tissues were removed, weighed, and macerated with scissors. Specific DiD tissue fluorescence for each organ was quantified using the IVIS Spectrum imaging system, and the mean percentage of injected dose per gram of tissue (% ID/g) was calculated as the final readout. Summarized statistics are displayed (n = 3, mean ± SEM; *p < 0.05; **p < 0.01; ***p < 0.001) (A, C, and E), and images of the tumors from each of the three mice for cMLV(DiD) and CAR.NK.cMLV(DiD) are shown (B, D, and F). NS, not significant.

significantly slowed tumor growth compared with CAR.NK and CAR.NK + cMLV(PTX) groups as well ($p < 0.05$ and $p < 0.01$, respectively; Figure 5). These data support the hypothesis that both immunotherapeutic effects from the NK cells and chemotherapeutic effects from the PTX play a role in the killing of tumor cells, as either component alone was not as effective as when the two were combined. Furthermore, even the mice treated with CAR.NK + cMLV(PTX) did not have as great an antitumor response as did the mice treated with CAR.NK.cMLV(PTX). This demonstrates that the physical conjugation between the drug and the NK cell is crucial to receiving the full benefits of the treatment system, and that the CAR.NK cells are facilitating the delivery of PTX to the tumor site for enhanced anticancer effects.

CAR.NK.cMLV(PTX) Enhances PTX Delivery into Tumor Site

We performed ex vivo analysis of our mouse xenograft tumor model to support our hypothesis that CAR.NK cells facilitate PTX delivery into the tumor site. Using high-performance liquid chromatography (HPLC), we quantified the intratumoral PTX concentrations in mice treated with PTX, including the groups cMLV(PTX), CAR.NK + cMLV(PTX), and CAR.NK.cMLV(PTX). The conjugated group, CAR.NK.cMLV(PTX), had significantly higher PTX concentrations within the tumor tissue compared with the cMLV(PTX) or CAR.NK + cMLV(PTX) ($p < 0.01$ and $p < 0.001$, respectively; Figure 6A).

We also used confocal imaging to visualize and quantify apoptotic cells in tumor tissues fixed on glass slides. There were significantly fewer terminal deoxynucleotidyl transferase dUTP nick end labeling (TUNEL)$^+$ cells in the PBS group compared with any other treatment group ($p < 0.0001$). Notably, CAR.NK.cMLV(PTX)-treated tumors had the greatest degree of cell apoptosis, with significantly higher percentages of TUNEL$^+$ cells compared with any other treatment group ($p < 0.0001$), indicating synergistic efficacy induced by the

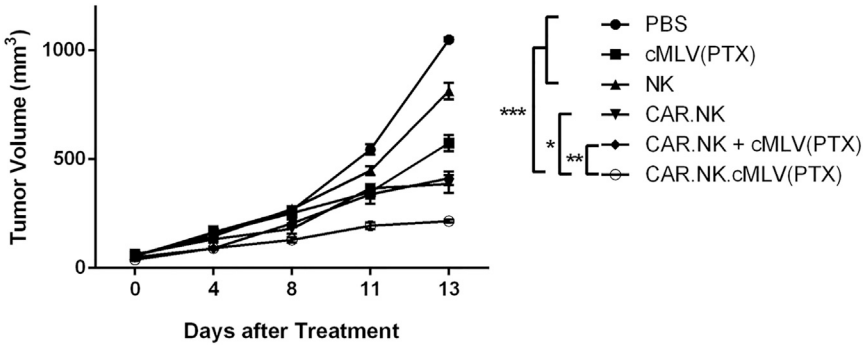

Figure 5. Antitumor Efficacy of CAR.NK.cMLV(PTX) in Solid Tumor Xenograft Model

Tumor growth curve. SKOV.CD19 cells were injected subcutaneously into the right flank of NSG mice on day 0. Mice were randomized into six groups (n = 5 per group) and treated according to their group description four times total, 3–4 days apart via tail-vein injection. Tumor size was measured with a fine caliper (n = 5; mean ± SEM; *p < 0.05; **p < 0.01; ***p < 0.001). NS, not significant.

co-localized delivery of the drug and CAR.NK cells (representative images are shown in Figure 6B; summarized data are shown in Figure 6C).

Finally, because the therapeutic effect of PTX is limited by its cardiotoxicity, slices of fixed heart tissue stained with H&E were imaged with light microscopy. Cardiotoxicity was defined as myofibrillary loss and disarray, as well as cytoplasmic vacuolization.[57] We observed no damage to the cardiac tissues in any of the treatment groups (Figure 6D). Because our delivery was targeted, we were able to use a very low dose of PTX (0.5 mg/kg) compared with those used in conventional PTX-based treatments,[57–59] thus resulting in minimal cardiotoxicity.

DISCUSSION

Our system combines nanoparticle-based drug delivery with immunotherapy to produce a cell-mediated, active targeting strategy. In vitro, we demonstrate that cMLV conjugation to NK cells does not trigger endocytosis, even though NK cells have phagocytotic capabilities.[60] The particles remain on the NK cell surface, perhaps in part because of the size of the cMLVs; previous studies have shown that surface-conjugated particles larger than 50 nm in diameter are not efficiently internalized.[61] Furthermore, the covalent linkage of maleimide-functionalized cMLVs to free thiols on immune cell surfaces has been shown to be stable for days after initial conjugation and even after cell division.[35] While the exact mechanisms of this prolonged surface retention remain to be discovered, the maleimide-thiol conjugation strategy has been shown to be a promising method of immune cell surface engineering.

We also have demonstrated in vitro that CAR.NK cells can specifically kill antigen-expressing cancer cells, that cMLV conjugation does not adversely affect NK cell function, and that conjugation of cMLV(PTX) to CAR.NK cells further augments cytotoxicity. While many studies of CAR.NK cells include results from cytotoxicity assays, but not from cytokine release assays,[21,22,53,62–64] we show that CAR.NK cells release IFN-γ in response to TAA^+ target cells. Neither CAR.NK cells coincubated with TAA^- target cells nor nontransduced NK cells coincubated with any target cells release IFN-γ. These results indicate that the enhanced cytotoxicity of CAR.NK cells was accompanied by an increase in IFN-γ release. In addition to sensitizing tumor cells to NK cytotoxicity,[65] IFN-γ release by both primary NK cells and NK cell lines[66] signals to surrounding immune cells, including T cells, dendritic cells, monocytes, and macrophages, initiating broader adaptive and innate immune responses.[67,68]

Our in vivo biodistribution study further supports that CAR.NK cells enhance nanoparticle accumulation within the tumor site. Mice treated with cMLV(DiD) without a cell chaperone had significantly greater cMLV accumulation in the liver, likely indicating hepatic clearance as commonly observed with larger liposomes.[55] However, the CAR.NK.cMLV(DiD)-treated mice had significantly greater cMLV accumulation at the tumor site. Additionally, significantly higher signal was observed in organs to which NK cells naturally home, such as the spleen and lymph nodes.[69] Our in vivo and ex vivo data provide evidence that CAR.NK cells facilitate the delivery of the chemotherapeutic drug PTX to the tumor site, slowing tumor growth and increasing intratumoral PTX concentrations more effectively than any other treatment group, including coadministered, but not conjugated, CAR.NK and cMLV(PTX). Finally, we were able to use a low dose of PTX and did not observe any cardiotoxicity.

We found that certain doses of PTX can kill tumor cells, but not NK92 cells, creating a therapeutic window in which we can use NK92 cells to deliver this chemotherapeutic drug to kill tumor cells, but not the carrier cells. However, we do not believe that this system is limited to PTX delivery. For example, murine T cells have been shown to deliver the anticancer drug SN-38 to lymphoma sites in vivo using drug-loaded nanocapsules conjugated to the cell surface. SN-38 effectively killed lymphoma cells but was not toxic to the T cell carriers.[4] Another study demonstrated that primary human T cells can enhance antitumor immune responses using surface-conjugated liposomes carrying the proinflammatory cytokines IL-15 and IL-21.[35] Surface engineering of immune cells has allowed a number of drugs or adjuvants to be delivered to the tumor site. To our knowledge, we present the first study of surface-engineered NK cells, as well as the first study using CAR.NK cells for tumor-targeted drug delivery. We believe that our CAR.NK-mediated drug delivery system can be expanded to include not only the delivery of traditional chemotherapeutic agents, but other anticancer treatments such as immunomodulators and small molecules that affect the tumor microenvironment.

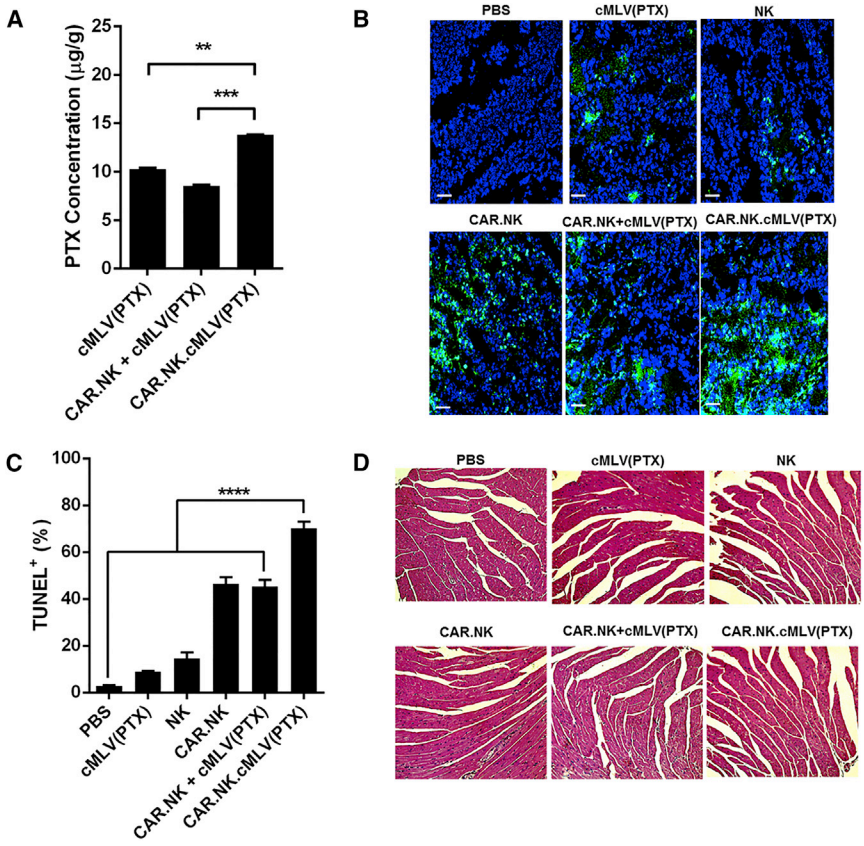

Figure 6. Ex Vivo Analysis of CAR.NK.cMLV(PTX) Treatment

(A) Intratumoral PTX concentration. Thawed tumor samples were homogenized and PTX concentrations were analyzed using HPLC (n = 3; mean ± SEM). (B) TUNEL assay of fixed frozen tumor sections. Tumor sections were stained with a TUNEL kit according to the manufacturer's instructions and imaged with confocal microscopy. Representative images are shown herein. Scale bars, 50 μm. (C) Quantification of TUNEL$^+$ cells from fixed frozen tumor sections (n = 16; mean ± SEM). (D) Histology slides for cardiac toxicity. Cardiac tissue was fixed and frozen, and sections were mounted on glass slides. The frozen sections were stained with H&E. Histopathologic specimens were examined by light microscopy. Representative images are shown herein. **p < 0.01; ***p < 0.001; ****p < 0.0001. NS, not significant.

Cancer immunotherapy has attracted much attention as an alternative or addition to chemotherapy, and currently a few clinical trials are using CAR-engineered T (CAR-T) cells to target patients with relapsed solid cancers, such as pancreatic, ovarian, prostate, and lung cancers.[16] However, CAR-T therapy relies on the ex vivo expansion of the patient's autologous T cells, which presents logistical issues and delays the start of the treatment while cells are in preparation (typically 2–3 weeks for the expansion of CAR-engineered immune cells for clinical use). These issues could be ameliorated in part by using an allogenic cell line instead of autologous cells; although few functional cytotoxic T cell lines are available, there are several functional, immortal NK cell lines. Of these NK cell lines, NK92 is the most promising and the only NK cell line used in clinical trials.[70]

There are a number of potential benefits to using CAR-engineered NK92 cells over CAR-T cells. CAR-engineered NK92 cells may provide an alternative "off-the-shelf" vehicle for CAR-based therapy, as well as provide more targeted drug delivery to the tumor site through surface engineering. NK92 cells double every 2–4 days, allowing for easy expansion, modification, and storage under good manufacturing practice (GMP) conditions. NK92 cells are identical to the parental cell line, eliminating problems with donor variability. There would be no lag time required for the ex vivo expansion and modification of autologous immune cells, which is especially crucial in patients with aggressive cancers, where a treatment delay of days to weeks could impact outcome.[51] NK92 cells are safe to use clinically if irradiated, which prevents proliferation. This decreases the risk of off-target effects compared with CAR-T cells. Short-lived CAR-engineered NK92 cells can be treated as a "living drug," redosing as necessary. Finally, allogenic NK92 cell-based therapies are less expensive than autologous CAR-T cell therapies[70]; one group estimated that each CAR-T protocol costs upward of $250,000 per patient, but NK92 cells used in the clinic cost around $20,000 per patient.[51]

In conclusion, we have demonstrated that CAR.NK cells conjugated to PTX-loaded cMLVs offer targeted drug delivery and improved antitumor efficacy. We believe that targeted drug delivery using surface-engineered CAR.NK cells is widely applicable, because both the CAR target and the drug payload potentially can be altered to treat a variety of cancer types. Overall, this study shows a promising combination of immunotherapy and drug delivery for enhanced antitumor treatment.

MATERIALS AND METHODS

Cell Lines and Reagents

MDA.MB.468 (ATCC HTB-132) and SKOV3 (ATCC HTB-77) tumor cell lines were maintained in a 5% CO_2 environment in RPMI 1640 (GIBCO) media supplemented with 10% fetal bovine serum (FBS), 1% penicillin-streptomycin (pen-strep), and 2 mM L-glutamine. NK92 cells (ATCC CRL-2407; Dr. Jihane Khalife, Children's Hospital Los Angeles) were maintained in MEM-α (GIBCO) supplemented with 10% FBS, 10% horse serum, 1% non-essential amino acid (NEAA), 1% pen-strep, 1% sodium pyruvate, 0.1 mM 2-β-mercaptoethanol, 0.2 mM myo-inositol, and 2.5 μM folic acid. CD19$^+$ SKOV3 (SKOV.CD19) cells were generated by transducing SKOV3

cells with lentivirus containing CD19 cDNA and sorting $CD19^+$ cells with fluorescence-activated cell sorting (FACS).

PTX was purchased from Sigma-Aldrich (St. Louis, MO, USA). All lipids were purchased from NOF Corporation (Japan): 1,2-dioleoyl-sn-glycero-3- phosphocholine (DOPC), 1,2-dioleoyl-sn-glycero-3-phospho-(10-rac-glycerol) (DOPG), and 1,2-dioleoyl-sn-glycero-3-phosphoethanolamine-N-[4-(p-maleimidophenyl)but-yramide (maleimide-head group lipid, MPB-PE).

Synthesis of Nanoparticles

Liposomes were prepared based on the conventional dehydration-rehydration method.[46,71] cMLVs were prepared from 1.5 μmol of lipids DOPC:DOPG:MPE-PE = 40:10:50 mixed in chloroform and evaporated under argon gas before drying under a vacuum overnight to form dried lipid films. The lipid film was rehydrated in 10 mM Bis-Tris propane at pH 7. After the lipid was mixed through vigorous vortexing every 10 min for 1 hr, they underwent three cycles of 15 s sonication (Microson XL2000; Misonix, Farmingdale, NY, USA) and rested on ice at 1 min intervals after each cycle. A final concentration of 10 mM $MgCl_2$ was added to induce divalent-triggered vesicle fusion. The cross-linking of multilamellar vesicles (cMLVs) was performed by addition of DTT (Sigma-Aldrich) at a final concentration of 1.5 mM for 1 hr at 37°C. The cMLVs were collected by centrifugation at 14,000 × *g* for 5 min and washed twice with PBS. The particles were suspended in filtered water, vortexed, and sonicated prior to analysis. Morphologic analysis of the multilamellar structure of vesicles was performed and confirmed by cryo-electron microscopy in previous studies.[46] As shown previously,[39] the hydrodynamic size of cMLVs was measured by dynamic light scattering (Wyatt Technology, Santa Barbara, CA, USA).

In Vitro Drug Encapsulation and Release

As previously reported,[57] the amount of incorporated PTX in the cMLV(PTX) was determined by C18 reverse-phase HPLC (RPHPLC) (Beckman Coulter, Brea, CA, USA). The cMLV(PTX) suspension was diluted by adding water and acetonitrile to a total volume of 0.5 mL. Extraction of PTX was accomplished by adding 5 mL of tert-butyl methyl ether and vortex-mixing the sample for 1 min. The mixtures were centrifuged, and the organic layer was transferred into a glass tube and evaporated under argon. Buffer A (95% water, 5% acetonitrile) was used to rehydrate the glass tube. To test PTX concentration, we injected 1 mL of the solution into a C18 column, and the PTX was detected at 227 nm (flow rate 1 mL/min). To obtain the release kinetics of PTX from cMLVs before and after cell conjugation, cMLV(PTX) and CAR.NK.cMLV(PTX) were incubated in 10% FBS-containing media at 37°C and were spun down and resuspended with fresh media daily. The PTX was quantified from the removed media by HPLC every day.

Nanoparticle Conjugation with Cells and In Situ PEGylation

Chemical conjugation of cMLVs to the cells was performed based on a method provided in previous studies.[4,35] We resuspended 10×10^6 cells/mL in serum-free MEM-α (GIBCO) medium. Equal volumes of nanoparticles were resuspended in nuclease-free water at different cMLV-to-NK cell conjugation ratios and incubated at 37°C. The cells and nanoparticles were mixed every 10 min for 30 min. After a PBS wash to remove unbound cMLVs from cells, cells were further incubated with 1 mg/mL thiol-terminated 2-kDa polyethylene glycol (PEG) at 37°C for 30 min in media to quench residual maleimide groups on cell-bound particles. We performed two PBS washes to remove unbound PEG. For quantification of cell-bound particles, particles were fluorescently labeled with the lipid-like fluorescent dye DiD (Invitrogen). Particle fluorescence was detected with flow cytometry and a fluorescent microplate reader. cMLVs were labeled with the lipid-like dye DiD, and CAR.NK cells were stained with carboxyfluorescein succinimidyl ester (CFSE) (Invitrogen), which allowed the conjugation of cMLVs to NK cells to be easily detected using confocal microscopy.

Lentiviral and Retroviral Production and Transduction of NK92 Cells

Our anti-Her2 CAR construct[42] was cloned into a lentiviral pCCW vector (a pCCL vector[43–45] with an additional WPRE region). The CAR consisted of the anti-Her2 scFv 4D5, a CD8 hinge and transmembrane region, and CD28, 4-1BB, and CD3ζ cytoplasmic regions. Our anti-CD19 CAR construct was cloned into an MP-71 retroviral vector backbone[41] and contained an anti-CD19 scFv, a CD8 hinge and transmembrane region, and CD28 and CD3ζ cytoplasmic regions. These plasmids were used to transfect HEK293T cells in 30 mL plates using $CaCl_2$ precipitation methods. Fresh media (high-glucose DMEM supplemented with 10% FBS and 1% pen-strep) was plated onto the cells 4 hr after initial transfection. Supernatants were harvested and filtered (0.45 μm) 48 hr later. NK92 cells were transduced with fresh retrovirus. Lentiviral supernatant was concentrated (25,000 rpm for 90 min at 4°C), resuspended in HBSS, and frozen at −80°C until later use. NK92 cells were transduced with concentrated lentivirus at MOI 40; the titer was based on transduction of 293T cells.

CAR Detection on NK Cell Surface

Three days after transduction, anti-CD19 CAR.NK cells (1×10^5) were incubated with biotinylated Protein L (PeproTech) at a volume ratio of 1:50 in PBS + 4% FBS at 4°C for 45 min and rinsed with PBS. The cells were subsequently incubated with streptavidin conjugated to FITC (BioLegend) at a volume ratio of 1:500 in PBS + 4% FBS at 4°C for 10 min, rinsed twice, and read using flow cytometry. Anti-Her2 CAR.NK cells (1×10^5) were incubated with rhHer2-Fc chimera (PeproTech) at a volume ratio of 1:50 (2 μg/mL) in PBS at 4°C for 30 min and rinsed with PBS. The cells were subsequently incubated with PE-labeled goat anti-human Fc (Jackson ImmunoResearch) at a volume ratio of 1:150 in PBS at 4°C for 10 min, rinsed, and read using flow cytometry. Nontransduced NK cells served as a negative control.

Internalization Assay

Quantification of cell cMLV internalization was performed based on a method previously described.[4,35] NK and CAR.NK cells were

conjugated with 5 mol% 18:1 PE CF [1,2-dioleoyl-sn-glycero-3-phosphoethanolamine-*N*-(carboxyfluorescein) (ammonium salt)] (Avanti; Polar Lipids)-tagged liposomes. After two PBS washes, cells were transferred to fibronectin (10 μg/mL)-coated 96-well plates. After a 2 hr incubation time, half of the wells were treated with 100 μL trypan blue in HBSS (0.25 mg/mL), an extracellular fluorescence quenching dye, for 1 min in order to differentiate between membrane-bound and internalized liposomes. Trypan blue was removed by gentle vacuum aspiration, and the cell uptake of liposomes was quantified by a fluorescence plate reader.

Cytokine Release Assay

NK cells (1×10^5 per well) were coincubated with target cells in 96-well plates at a 1:1 ratio for 6 hr at 37°C. 1 μg of brefeldin A (Sigma) was added to each well to prevent protein transport. At the end of the incubation, cells were permeabilized using the Cytofix/Cytoperm kit (BD Biosciences) and stained for CD8 and IFN-γ using Pacific Blue-conjugated anti-human CD8 (BioLegend) and PE-conjugated anti-human IFN-γ (BioLegend). Unstimulated cells served as a negative control. Results were read using flow cytometry.

Cytotoxicity Assay

Target cells (1×10^4) were labeled with 5 μM CFSE (Life Technologies) as previously described[72] and coincubated with NK cells at various ratios in 96-well plates for 24 hr at 37°C. The cells were then incubated in 7-aminoactinomycin D (7-AAD; Life Technologies) in PBS (1:1,000 dilution) for 10 min at room temperature and analyzed via flow cytometry. Percentages of killed cells were calculated as $CFSE^+7\text{-}AAD^+$ cells/($CFSE^+7\text{-}AAD^- + CFSE^+7\text{-}AAD^+$) cells, with live/dead gates based on control wells of target cells to account for spontaneous cell death.

NK92 and SKOV3 cells were seeded in 96-well plates at 2×10^4 cells per well in 10% FBS-containing media and grown at 37°C in the presence of 5% CO_2 for 6 hr. Cells were incubated with various concentrations of cMLV (PTX) as previously described,[57] and cell viability was assessed using the Cell Proliferation Kit II (XTT assay) from Roche Applied Science (Indianapolis, IN, USA) according to the manufacturer's instructions. Cell viability percentage was determined by subtracting absorbance values obtained from media-only wells from the treated wells and then normalized by the control wells containing cells without drugs.

Transmigration Assay

NK cell transmigration assays were performed in 24-mm-diameter 3-μm-pore size Transwell plates (Costar). NK cells either conjugated or unconjugated to cMLVs were plated on the upper wells, and media were added to the lower wells. The chemoattractant CXCL9 (0.1 mg/mL; PeproTech) was added to the lower wells. After incubation at 37°C for 6 hr, NK cells that had migrated into the lower chamber were counted.

In Vivo Biodistribution Study

Female 6- to 10-week-old NOD.Cg-$Prkdc^{SCID}IL2R\gamma^{tm1Wjl}$/SZ (NSG) mice were purchased from Jackson Laboratories (Bar Harbor, ME, USA). All mice were held under specific pathogen-reduced conditions in the animal facility of the University of Southern California (Los Angeles, CA, USA). All experiments were performed in accordance with the guidelines set by the NIH and the University of Southern California on the Care and Use of Animals. A total of 3.5×10^6 SKOV3.CD19 cells was inoculated subcutaneously into the flanks of NOD/SCID/IL2r$\gamma^{-/-}$ (NSG) mice on day −14, and tumors were allowed to grow until they reached 100 mm^3. On day 0, mice were injected intravenously through the tail vein with either cMLV(DiD) or CAR.NK.cMLV(DiD). 24, 48, and 72 hr after injection, mice were sacrificed and organs were analyzed for fluorescence intensity. DiD tissue fluorescence for each organ was quantified using the IVIS Spectrum imaging system, and the percentage of injected dose per gram of tissue (%ID/g) was calculated.

Xenograft Tumor Model

A total of 3.5×10^6 SKOV3.CD19 cells was inoculated subcutaneously into the flanks of NSG mice on day −14, and tumors were allowed to grow to 70–100 mm^3. Mice were randomly divided into six groups of five mice each. On days 0, 4, 7, and 11, the mice were injected intravenously through the tail vein with either PBS, cMLV(PTX) only, nontransduced NK cells only, CAR.NK cells only, mixed CAR.NK + cMLV(PTX), which were not conjugated together, or conjugated CAR.NK.cMLV(PTX). 5×10^6 cells per mouse were injected each time in the groups that were given NK cells. Tumor growth and body weight of the mice were recorded until sacrifice. The tumor length and width were measured with a fine caliper, and tumor volume was calculated as $1/2 \times (\text{length}) \times (\text{width})^2$.

Intratumoral PTX Concentration Measurements Ex Vivo

Using HPLC, we quantified the PTX concentration in the frozen tumor tissues as previously detailed.[39] Briefly, thawed tumor tissues were chopped and homogenized in ethyl acetate, with a known concentration of docetaxel added to each sample as an internal standard. The samples were centrifuged, and the organic layer was transferred to a clean tube. The organic layer was evaporated under a stream of argon and rehydrated in diluted acetonitrile. After running the samples on HPLC, the peak heights were analyzed to determine intratumoral PTX concentration.

Immunohistochemistry of Tumors, Cardiac Toxicity, and Confocal Imaging

Tumors were excised, fixed, frozen, cryo-sectioned, and mounted onto glass slides. Frozen sections were fixed and rinsed with cold PBS. After blocking and permeabilization, the slides were washed with PBS and incubated with a terminal deoxynucleotidyl transferase dUTP nick end labeling (TUNEL) reaction mixture (Roche, Indianapolis, IN, USA) for 1 hr and counterstained with DAPI (Invitrogen, Carlsbad, CA, USA). Fluorescence images were acquired by a Yokogawa spinning-disk confocal scanner system (Solamere Technology Group, Salt Lake City, UT, USA) using a Nikon Eclipse Ti-E microscope. Illumination powers at 405, 491, 561, and 640 nm solid-state laser lines were provided by an AOTF (acousto-optical tunable filter)-controlled laser-merge system with 50 mW for each laser. All

images were analyzed using Nikon NIS-Elements software. For quantifying TUNEL-positive cells, four regions of interest (ROIs) were randomly chosen per image at ×10 magnification. Within one region, the area of TUNEL-positive nuclei and the area of nuclear staining were counted by Nikon NIS-Element software, with data expressed as percentage total nuclear area stained by TUNEL in the region. For cardiac toxicity, heart tissues were harvested 2 days after the last injection and were fixed in 4% formaldehyde. The tissues were frozen and then cut into sections and mounted onto glass slides. The frozen sections were stained with H&E. Histopathologic specimens were examined by EVOS light microscopy.

Statistics

The differences between two groups were determined with Student's t test. The differences among three or more groups were determined with a one-way ANOVA.

SUPPLEMENTAL INFORMATION

Supplemental Information includes five figures and can be found with this article online at http://dx.doi.org/10.1016/j.ymthe.2017.08.010.

AUTHOR CONTRIBUTIONS

E.L.S. and Y.J.K. designed, performed, and analyzed experiments and wrote the manuscript. X.C. contributed to the production and culture of anti-CD19 CAR.NK cells. N.S. provided support with in vivo experiments. J.M. optimized and performed HPLC experiments. J.A.R. helped to edit the manuscript. P.D.B. provided the anti-Her2 CAR construct. P.W. devised the initial concept and supervised the work.

CONFLICTS OF INTEREST

The authors certify that they have no affiliations with or involvement in any organization or entity with any financial interest or non-financial interest in the subject matter or materials discussed in this manuscript.

ACKNOWLEDGMENTS

We thank Dr. Jihane Khalife at the Children's Hospital Los Angeles for providing the NK92 cell culture protocol. This work was supported by National Institutes of Health grants R01AI068978, R01CA170820, R01EB017206, and P01CA132681 and a translational acceleration grant from the Joint Center for Translational Medicine.

REFERENCES

1. Sudhakar, A. (2009). History of cancer, ancient and modern treatment methods. J. Cancer Sci. Ther. *1*, 1–4.
2. Gottesman, M.M. (2002). Mechanisms of cancer drug resistance. Annu. Rev. Med. *53*, 615–627.
3. Armstrong, D.K. (2002). Relapsed ovarian cancer: challenges and management strategies for a chronic disease. Oncologist *7* (*Suppl 5*), 20–28.
4. Huang, B., Abraham, W.D., Zheng, Y., Bustamante López, S.C., Luo, S.S., and Irvine, D.J. (2015). Active targeting of chemotherapy to disseminated tumors using nanoparticle-carrying T cells. Sci. Transl. Med. *7*, 291ra94.
5. Mitchell, M.J., and King, M.R. (2015). Leukocytes as carriers for targeted cancer drug delivery. Expert Opin. Drug Deliv. *12*, 375–392.
6. Kennedy, L.C., Bear, A.S., Young, J.K., Lewinski, N.A., Kim, J., Foster, A.E., and Drezek, R.A. (2011). T cells enhance gold nanoparticle delivery to tumors in vivo. Nanoscale Res. Lett. *6*, 283.
7. Rezvani, K., and Rouce, R.H. (2015). The application of natural killer cell immunotherapy for the treatment of cancer. Front. Immunol. *6*, 578.
8. Pittari, G., Filippini, P., Gentilcore, G., Grivel, J.C., and Rutella, S. (2015). Revving up natural killer cells and cytokine-induced killer cells against hematological malignancies. Front. Immunol. *6*, 230.
9. Gong, J.H., Maki, G., and Klingemann, H.G. (1994). Characterization of a human cell line (NK-92) with phenotypical and functional characteristics of activated natural killer cells. Leukemia *8*, 652–658.
10. Ames, E., and Murphy, W.J. (2014). Advantages and clinical applications of natural killer cells in cancer immunotherapy. Cancer Immunol. Immunother. *63*, 21–28.
11. Tonn, T., Schwabe, D., Klingemann, H.G., Becker, S., Esser, R., Koehl, U., Suttorp, M., Seifried, E., Ottmann, O.G., and Bug, G. (2013). Treatment of patients with advanced cancer with the natural killer cell line NK-92. Cytotherapy *15*, 1563–1570.
12. Hwang, M.H., Li, X.J., Kim, J.E., Jeong, S.Y., Lee, S.W., Lee, J., and Ahn, B.C. (2015). Potential therapeutic effect of natural killer cells on doxorubicin-resistant breast cancer cells in vitro. PLoS ONE *10*, e0136209.
13. Cheng, M., Chen, Y., Xiao, W., Sun, R., and Tian, Z. (2013). NK cell-based immunotherapy for malignant diseases. Cell. Mol. Immunol. *10*, 230–252.
14. Dai, H., Wang, Y., Lu, X., and Han, W. (2016). Chimeric antigen receptors modified T-cells for cancer therapy. J. Natl. Cancer Inst. *108*, djv439.
15. Barrett, D.M., Singh, N., Porter, D.L., Grupp, S.A., and June, C.H. (2014). Chimeric antigen receptor therapy for cancer. Annu. Rev. Med. *65*, 333–347.
16. Fesnak, A.D., June, C.H., and Levine, B.L. (2016). Engineered T cells: the promise and challenges of cancer immunotherapy. Nat. Rev. Cancer *16*, 566–581.
17. Lee, D.W., Kochenderfer, J.N., Stetler-Stevenson, M., Cui, Y.K., Delbrook, C., Feldman, S.A., Fry, T.J., Orentas, R., Sabatino, M., Shah, N.N., et al. (2015). T cells expressing CD19 chimeric antigen receptors for acute lymphoblastic leukaemia in children and young adults: a phase 1 dose-escalation trial. Lancet *385*, 517–528.
18. Sadelain, M., Brentjens, R., and Rivière, I. (2013). The basic principles of chimeric antigen receptor design. Cancer Discov. *3*, 388–398.
19. Long, A.H., Haso, W.M., Shern, J.F., Wanhainen, K.M., Murgai, M., Ingaramo, M., Smith, J.P., Walker, A.J., Kohler, M.E., Venkateshwara, V.R., et al. (2015). 4-1BB costimulation ameliorates T cell exhaustion induced by tonic signaling of chimeric antigen receptors. Nat. Med. *21*, 581–590.
20. Han, J., Chu, J., Keung Chan, W., Zhang, J., Wang, Y., Cohen, J.B., Victor, A., Meisen, W.H., Kim, S.H., Grandi, P., et al. (2015). CAR-engineered NK cells targeting wild-type EGFR and EGFRvIII enhance killing of glioblastoma and patient-derived glioblastoma stem cells. Sci. Rep. *5*, 11483.
21. Liu, H., Yang, B., Sun, T., Lin, L., Hu, Y., Deng, M., Yang, J., Liu, T., Li, J., Sun, S., and Jiao, S. (2015). Specific growth inhibition of ErbB2-expressing human breast cancer cells by genetically modified NK-92 cells. Oncol. Rep. *33*, 95–102.
22. Schönfeld, K., Sahm, C., Zhang, C., Naundorf, S., Brendel, C., Odendahl, M., Nowakowska, P., Bönig, H., Köhl, U., Kloess, S., et al. (2015). Selective inhibition of tumor growth by clonal NK cells expressing an ErbB2/HER2-specific chimeric antigen receptor. Mol. Ther. *23*, 330–338.
23. Glienke, W., Esser, R., Priesner, C., Suerth, J.D., Schambach, A., Wels, W.S., Grez, M., Kloess, S., Arseniev, L., and Koehl, U. (2015). Advantages and applications of CAR-expressing natural killer cells. Front. Pharmacol. *6*, 21.
24. Ma, P., and Mumper, R.J. (2013). Paclitaxel nano-delivery systems: a comprehensive review. J. Nanomed. Nanotechnol. *4*, 1000164.
25. Zou, H., Li, L., Garcia Carcedo, I., Xu, Z.P., Monteiro, M., and Gu, W. (2016). Synergistic inhibition of colon cancer cell growth with nanoemulsion-loaded paclitaxel and PI3K/mTOR dual inhibitor BEZ235 through apoptosis. Int. J. Nanomedicine *11*, 1947–1958.
26. Xiong, W., Peng, L., Chen, H., and Li, Q. (2015). Surface modification of MPEG-b-PCL-based nanoparticles via oxidative self-polymerization of dopamine for malignant melanoma therapy. Int. J. Nanomedicine *10*, 2985–2996.

27. Prabhakar, U., Maeda, H., Jain, R.K., Sevick-Muraca, E.M., Zamboni, W., Farokhzad, O.C., Barry, S.T., Gabizon, A., Grodzinski, P., and Blakey, D.C. (2013). Challenges and key considerations of the enhanced permeability and retention effect for nanomedicine drug delivery in oncology. Cancer Res. *73*, 2412–2417.

28. Greish, K. (2010). Enhanced permeability and retention (EPR) effect for anticancer nanomedicine drug targeting. Methods Mol. Biol. *624*, 25–37.

29. Clark, A.J., Wiley, D.T., Zuckerman, J.E., Webster, P., Chao, J., Lin, J., Yen, Y., and Davis, M.E. (2016). CRLX101 nanoparticles localize in human tumors and not in adjacent, nonneoplastic tissue after intravenous dosing. Proc. Natl. Acad. Sci. USA *113*, 3850–3854.

30. Stephan, M.T., and Irvine, D.J. (2011). Enhancing cell therapies from the outside in: cell surface engineering using synthetic nanomaterials. Nano Today *6*, 309–325.

31. Jang, E.S., Shin, J.H., Ren, G., Park, M.J., Cheng, K., Chen, X., Wu, J.C., Sunwoo, J.B., and Cheng, Z. (2012). The manipulation of natural killer cells to target tumor sites using magnetic nanoparticles. Biomaterials *33*, 5584–5592.

32. Cole, C., Qiao, J., Kottke, T., Diaz, R.M., Ahmed, A., Sanchez-Perez, L., Brunn, G., Thompson, J., Chester, J., and Vile, R.G. (2005). Tumor-targeted, systemic delivery of therapeutic viral vectors using hitchhiking on antigen-specific T cells. Nat. Med. *11*, 1073–1081.

33. Russell, S.J., and Peng, K.W. (2008). The utility of cells as vehicles for oncolytic virus therapies. Curr. Opin. Mol. Ther. *10*, 380–386.

34. Ilett, E.J., Prestwich, R.J., Kottke, T., Errington, F., Thompson, J.M., Harrington, K.J., Pandha, H.S., Coffey, M., Selby, P.J., Vile, R.G., and Melcher, A.A. (2009). Dendritic cells and T cells deliver oncolytic reovirus for tumour killing despite pre-existing anti-viral immunity. Gene Ther. *16*, 689–699.

35. Stephan, M.T., Moon, J.J., Um, S.H., Bershteyn, A., and Irvine, D.J. (2010). Therapeutic cell engineering with surface-conjugated synthetic nanoparticles. Nat. Med. *16*, 1035–1041.

36. Zheng, Y., Stephan, M.T., Gai, S.A., Abraham, W., Shearer, A., and Irvine, D.J. (2013). In vivo targeting of adoptively transferred T-cells with antibody- and cytokine-conjugated liposomes. J. Control. Release *172*, 426–435.

37. Irvine, D.J., Hanson, M.C., Rakhra, K., and Tokatlian, T. (2015). Synthetic nanoparticles for vaccines and immunotherapy. Chem. Rev. *115*, 11109–11146.

38. Thorén, F.B., Romero, A.I., Hermodsson, S., and Hellstrand, K. (2007). The CD16-/CD56bright subset of NK cells is resistant to oxidant-induced cell death. J. Immunol. *179*, 781–785.

39. Liu, Y., Fang, J., Joo, K.I., Wong, M.K., and Wang, P. (2014). Codelivery of chemotherapeutics via crosslinked multilamellar liposomal vesicles to overcome multidrug resistance in tumor. PLoS ONE *9*, e110611.

40. Kim, Y.J., Liu, Y., Li, S., Rohrs, J., Zhang, R., Zhang, X., and Wang, P. (2015). Co-eradication of breast cancer cells and cancer stem cells by cross-linked multilamellar liposomes enhances tumor treatment. Mol. Pharm. *12*, 2811–2822.

41. Engels, B., Cam, H., Schüler, T., Indraccolo, S., Gladow, M., Baum, C., Blankenstein, T., and Uckert, W. (2003). Retroviral vectors for high-level transgene expression in T lymphocytes. Hum. Gene Ther. *14*, 1155–1168.

42. Zhao, Y., Wang, Q.J., Yang, S., Kochenderfer, J.N., Zheng, Z., Zhong, X., Sadelain, M., Eshhar, Z., Rosenberg, S.A., and Morgan, R.A. (2009). A herceptin-based chimeric antigen receptor with modified signaling domains leads to enhanced survival of transduced T lymphocytes and antitumor activity. J. Immunol. *183*, 5563–5574.

43. Haas, D.L., Lutzko, C., Logan, A.C., Cho, G.J., Skelton, D., Jin Yu, X., Pepper, K.A., and Kohn, D.B. (2003). The Moloney murine leukemia virus repressor binding site represses expression in murine and human hematopoietic stem cells. J. Virol. *77*, 9439–9450.

44. Dull, T., Zufferey, R., Kelly, M., Mandel, R.J., Nguyen, M., Trono, D., and Naldini, L. (1998). A third-generation lentivirus vector with a conditional packaging system. J. Virol. *72*, 8463–8471.

45. Logan, A.C., Nightingale, S.J., Haas, D.L., Cho, G.J., Pepper, K.A., and Kohn, D.B. (2004). Factors influencing the titer and infectivity of lentiviral vectors. Hum. Gene Ther. *15*, 976–988.

46. Joo, K.I., Xiao, L., Liu, S., Liu, Y., Lee, C.L., Conti, P.S., Wong, M.K., Li, Z., and Wang, P. (2013). Crosslinked multilamellar liposomes for controlled delivery of anticancer drugs. Biomaterials *34*, 3098–3109.

47. Yameen, B., Choi, W.I., Vilos, C., Swami, A., Shi, J., and Farokhzad, O.C. (2014). Insight into nanoparticle cellular uptake and intracellular targeting. J. Control. Release *190*, 485–499.

48. Voigt, J., Christensen, J., and Shastri, V.P. (2014). Differential uptake of nanoparticles by endothelial cells through polyelectrolytes with affinity for caveolae. Proc. Natl. Acad. Sci. USA *111*, 2942–2947.

49. Choi, C.H., Hao, L., Narayan, S.P., Auyeung, E., and Mirkin, C.A. (2013). Mechanism for the endocytosis of spherical nucleic acid nanoparticle conjugates. Proc. Natl. Acad. Sci. USA *110*, 7625–7630.

50. Champion, J.A., and Mitragotri, S. (2009). Shape induced inhibition of phagocytosis of polymer particles. Pharm. Res. *26*, 244–249.

51. Klingemann, H., Boissel, L., and Toneguzzo, F. (2016). Natural killer cells for immunotherapy –advantages of the NK-92 cell line over blood NK cells. Front. Immunol. *7*, 91.

52. Klingemann, H.G., Wong, E., and Maki, G. (1996). A cytotoxic NK-cell line (NK-92) for ex vivo purging of leukemia from blood. Biol. Blood Marrow Transplant. *2*, 68–75.

53. Boissel, L., Betancur, M., Wels, W.S., Tuncer, H., and Klingemann, H. (2009). Transfection with mRNA for CD19 specific chimeric antigen receptor restores NK cell mediated killing of CLL cells. Leuk. Res. *33*, 1255–1259.

54. Robertson, M.J. (2002). Role of chemokines in the biology of natural killer cells. J. Leukoc. Biol. *71*, 173–183.

55. Longmire, M., Choyke, P.L., and Kobayashi, H. (2008). Clearance properties of nano-sized particles and molecules as imaging agents: considerations and caveats. Nanomedicine (Lond.) *3*, 703–717.

56. Alexis, F., Pridgen, E., Molnar, L.K., and Farokhzad, O.C. (2008). Factors affecting the clearance and biodistribution of polymeric nanoparticles. Mol. Pharm. *5*, 505–515.

57. Liu, Y., Fang, J., Kim, Y.J., Wong, M.K., and Wang, P. (2014). Codelivery of doxorubicin and paclitaxel by cross-linked multilamellar liposome enables synergistic antitumor activity. Mol. Pharm. *11*, 1651–1661.

58. Cividalli, A., Cruciani, G., Livdi, E., Cordelli, E., Eletti, B., and Tirindelli Danesi, D. (1998). Greater antitumor efficacy of paclitaxel administered before epirubicin in a mouse mammary carcinoma. J. Cancer Res. Clin. Oncol. *124*, 236–244.

59. Galmarini, C.M., Bouchet, B.P., Falette, N., Vila, L., Lamblot, C., Audoynaud, C., Bertholon, J., and Puisieux, A. (2007). Weekly administration of paclitaxel induces long-term aneugenicity in nude mice. Cancer Biol. Ther. *6*, 377–382.

60. Aderem, A., and Underhill, D.M. (1999). Mechanisms of phagocytosis in macrophages. Annu. Rev. Immunol. *17*, 593–623.

61. Jiang, W., Kim, B.Y., Rutka, J.T., and Chan, W.C. (2008). Nanoparticle-mediated cellular response is size-dependent. Nat. Nanotechnol. *3*, 145–150.

62. Müller, T., Uherek, C., Maki, G., Chow, K.U., Schimpf, A., Klingemann, H.G., Tonn, T., and Wels, W.S. (2008). Expression of a CD20-specific chimeric antigen receptor enhances cytotoxic activity of NK cells and overcomes NK-resistance of lymphoma and leukemia cells. Cancer Immunol. Immunother. *57*, 411–423.

63. Schirrmann, T., and Pecher, G. (2005). Specific targeting of CD33(+) leukemia cells by a natural killer cell line modified with a chimeric receptor. Leuk. Res. *29*, 301–306.

64. Sahm, C., Schönfeld, K., and Wels, W.S. (2012). Expression of IL-15 in NK cells results in rapid enrichment and selective cytotoxicity of gene-modified effectors that carry a tumor-specific antigen receptor. Cancer Immunol. Immunother. *61*, 1451–1461.

65. Wang, R., Jaw, J.J., Stutzman, N.C., Zou, Z., and Sun, P.D. (2012). Natural killer cell-produced IFN-γ and TNF-α induce target cell cytolysis through up-regulation of ICAM-1. J. Leukoc. Biol. *91*, 299–309.

66. Ye, J., Ortaldo, J.R., Conlon, K., Winkler-Pickett, R., and Young, H.A. (1995). Cellular and molecular mechanisms of IFN-gamma production induced by IL-2 and IL-12 in a human NK cell line. J. Leukoc. Biol. *58*, 225–233.

67. Gross, E., Sunwoo, J.B., and Bui, J.D. (2013). Cancer immunosurveillance and immunoediting by natural killer cells. Cancer J. *19*, 483–489.

68. Gómez-Lomelí, P., Bravo-Cuellar, A., Hernández-Flores, G., Jave-Suárez, L.F., Aguilar-Lemarroy, A., Lerma-Díaz, J.M., Domínguez-Rodríguez, J.R., Sánchez-Reyes, K., and

Ortiz-Lazareno, P.C. (2014). Increase of IFN-γ and TNF-α production in CD107a + NK-92 cells co-cultured with cervical cancer cell lines pre-treated with the HO-1 inhibitor. Cancer Cell Int. *14*, 100.

69. Fehniger, T.A., Cooper, M.A., Nuovo, G.J., Cella, M., Facchetti, F., Colonna, M., and Caligiuri, M.A. (2003). CD56bright natural killer cells are present in human lymph nodes and are activated by T cell-derived IL-2: a potential new link between adaptive and innate immunity. Blood *101*, 3052–3057.

70. Liu, D., Tian, S., Zhang, K., Xiong, W., Lubaki, N., Chen, Z., and Han, W. (2017). Chimeric antigen receptor (CAR)-modified natural killer cell-based immunotherapy and immunological synapse formation in cancer and HIV. Protein Cell, Published online May 9, 2017. http://dx.doi.org/10.1007/s13238-017-0415-5.

71. Moon, J.J., Suh, H., Bershteyn, A., Stephan, M.T., Liu, H., Huang, B., Sohail, M., Luo, S., Um, S.H., Khant, H., et al. (2011). Interbilayer-crosslinked multilamellar vesicles as synthetic vaccines for potent humoral and cellular immune responses. Nat. Mater. *10*, 243–251.

72. Han, X., Bryson, P.D., Zhao, Y., Cinay, G.E., Li, S., Guo, Y., Siriwon, N., and Wang, P. (2017). Masked chimeric antigen receptor for tumor-specific activation. Mol. Ther. *25*, 274–284.